Growth of single-crystalline zirconium diboride thin film on sapphire

Sambhunath Bera,[a] Yuichiro Sumiyoshi, and Yukiko Yamada-Takamura[b]
School of Materials Science and Research Center for Integrated Science, Japan Advanced Institute of Science and Technology (JAIST), 1-1 Asahidai, Nomi, Ishikawa 923-1292 Japan

(Received 13 July 2009; accepted 20 August 2009; published online 25 September 2009)

Conducting and reflecting thin film of ZrB_2, which has lattice mismatch of only 0.6% to GaN, was grown epitaxially on sapphire substrate [α-$Al_2O_3(0001)$] via thermal decomposition of $Zr(BH_4)_4$. *In situ* reflection high energy electron diffraction and *ex situ* x-ray diffraction analyses indicate that the epitaxial relationship is singular, i.e., $ZrB_2[0001]\|Al_2O_3[0001]$ and $ZrB_2[11\bar{2}0]\|Al_2O_3[10\bar{1}0]$. X-ray photoelectron spectroscopy and scanning tunneling microscopy revealed that the oxide-free surface could be recovered by heating the film at approximately 750 °C under ultrahigh vacuum, which demonstrates its suitability as a template for the growth of nitride semiconductors. © *2009 American Institute of Physics*. [doi:10.1063/1.3226881]

I. INTRODUCTION

Group-III nitride (III-N) semiconductors with direct band gap are now the dominating materials for short-wavelength optoelectronic devices, such as light-emitting diodes, laser diodes, and photodetectors.[1] Sapphire has been the most commonly used substrate for the epitaxial growth of wurtzitic III-N, but since sapphire has large lattice mismatch (16%) and thermal expansion coefficient mismatch (27%) to GaN, buffer layers such as AlN (Ref. 2) or GaN (Ref. 3) grown at low temperature were crucial to achieve high quality III-N film. Recently, zirconium diboride (ZrB_2), which has a hexagonal AlB_2 structure, has been proposed as a lattice- (ZrB_2: a=3.169 Å, GaN: a=3.189 Å, 0.6% mismatch) and thermal expansion coefficient-matched (ZrB_2: 5.9×10^{-6} K^{-1}, GaN: 5.6×10^{-6} K^{-1} along $[10\bar{1}0]$ direction, 5.3% mismatch) and conductive (4.6 $\mu\Omega$ cm) substrate for III-N growth.[4] ZrB_2 is a very stable compound with high hardness and high melting temperature (3220 °C), which are desirable for III-N growth carried out under high growth temperature. If single-crystalline ZrB_2 layer could be grown on sapphire, the layer can serve as a lattice-matched buffer layer as well as thermally stable electrode. ZrB_2 thin film has been studied using various vapor deposition techniques,[5–7] because of its high expectation not only as wear-, heat-, and corrosion-resistant coatings but also as diffusion barrier[5] and thermally stable electrode in electronic devices,[6] especially, in high power devices.[7] These films were amorphous or polycrystalline, but recently, ZrB_2 has been epitaxially grown on Si(111) through 6:5 magic mismatch using thermal decomposition of $Zr(BH_4)_4$.[8] GaN was grown on this single-crystalline ZrB_2 film, and it was demonstrated that the lattice-matched growth template also acts as a metallic reflective layer, which prevents the loss of emitted light to silicon substrate.[8] In this letter, we demonstrate that epitaxial ZrB_2 layer with single crystal orientation, high crystallinity, and high conductivity could be grown on sapphire substrate using the thermal decomposition of $Zr(BH_4)_4$, and that the oxide layer formed by exposing the film to air can be removed by annealing in ultrahigh vacuum (UHV).

II. GROWTH PROCESS

ZrB_2 growth was carried out in a UHV system with base pressure of 1.0×10^{-8} Pa. The flow of $Zr(BH_4)_4$ vapor was adjusted by a leak valve, and delivered through a gas inlet capillary tube with inner diameter of 2.18 mm. The end of capillary was positioned 40 mm from the substrate. In order to grow epitaxial ZrB_2 film, the pressure of $Zr(BH_4)_4$ in the growth chamber was maintained as low as 7.0×10^{-5} Pa to sustain a slow growth rate of approximately 0.3 nm/min. 10-mm-square and 0.5-mm-thick c-plane sapphire single crystals, which were pretreated at high temperature for atomically flat terraces, were used as substrates.

We first describe the detail growth process of ZrB_2 epilayer based on *in situ* reflection high-energy electron diffraction (RHEED) observation. The evolution of RHEED pattern during the growth, shown in Fig. 1, was acquired for a sample grown at 1000 °C. The evolution was common among films grown with substrate temperature between 935 and 1040 °C. Figure 1(a) shows a set of RHEED patterns from sapphire substrate with electron beam parallel to $[10\bar{1}0]$ (left image) and $[11\bar{2}0]$ (right image) directions. The streaks indicate that the substrate is atomically smooth. After a few minutes after introducing $Zr(BH_4)_4$, spots corresponding to hexagonal $ZrB_2(0001)$ appeared with an in-plane epitaxial relationship of $ZrB_2[11\bar{2}0]\|Al_2O_3[10\bar{1}0]$, which was also verified by *ex situ* x-ray diffraction (XRD) and will be discussed later. After the nucleation and growth in three-dimensional mode, the growth mode changes into two-dimensional, i.e., spotty pattern converts into streaky [Figs. 1(b) and 1(c)] pattern. As a result, we were able to observe a well-defined $(\sqrt{3}\times\sqrt{3})$ reconstruction [Fig. 1(d)], which maintains throughout the growth process, and also after terminating the growth at 60 min and cooling down the sample to room temperature. This $(\sqrt{3}\times\sqrt{3})$ surface reconstruction is different from the ones observed during the growth of ZrB_2 film on Si(111), $ZrB_2(0001)$-(1×1) and (2×2),[9] sug-

[a]Present address: Laboratoire Interdisciplinaire sur l'Organisation Nanométrique et Supramoléculaire (LIONS), SIS2M-bát. 125, CEA Saclay, F-91191 Gif-sur Yvette, France.
[b]Author to whom correspondence should be addressed. Electronic mail: yukikoyt@jaist.ac.jp.

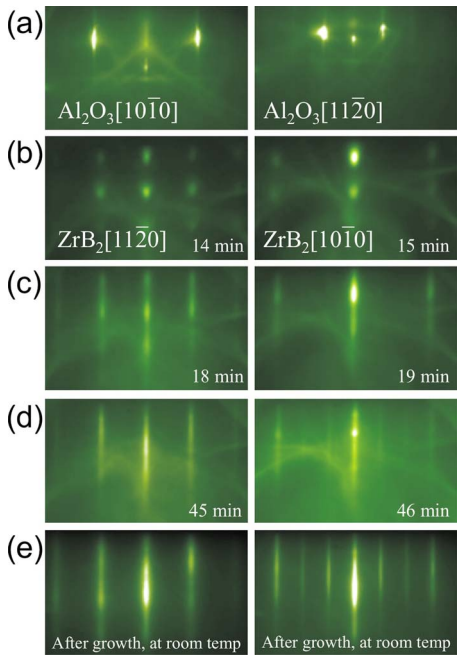

FIG. 1. (Color online) RHEED pattern evolution during the growth of ZrB_2 thin film on sapphire *c*-plane. Patterns in the same column were acquired at the same sample rotational angle. (a) Patterns along $[10\bar{1}0]$ (the left panel) and $[11\bar{2}0]$ (the right panel) electron-beam azimuths of the clean $Al_2O_3(0001)$ substrate prior to ZrB_2 growth. Patterns observed (b)–(d) during growth, and (e) after terminating the growth and cooling down to room temperature. The patterns in the left and the right columns of (b)–(e) corresponds to $ZrB_2(0001)$ pattern with electron-beam azimuth along $[11\bar{2}0]$ and $[10\bar{1}0]$, respectively. A well-defined $(\sqrt{3}\times\sqrt{3})$ reconstruction is observed during and after growth.

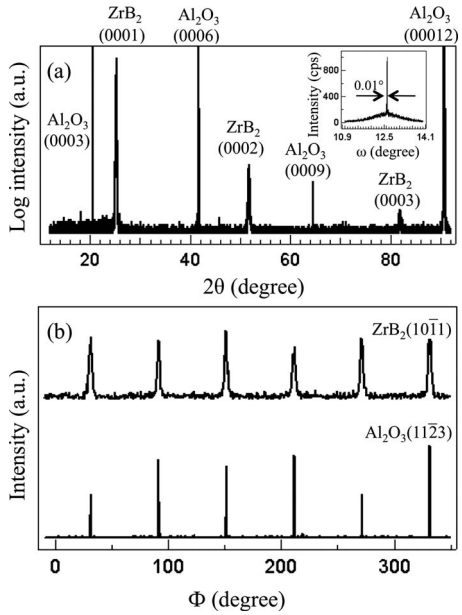

FIG. 2. (a) XRD (θ-2θ) scan of the $ZrB_2/Al_2O_3(0001)$ using triple axis optics. Inset figure: The rocking curve of the (0001) reflection of ZrB_2. (b) Φ scan of $(10\bar{1}1)$ reflection for ZrB_2 and $(11\bar{2}3)$ reflection for Al_2O_3 substrate. Peak spacing of 60° are visible for both film and substrate according to the sixfold symmetry of ZrB_2 and sapphire; the two crystals are rotated by 30° around *c*-axis with respect to each other.

gesting that these reconstructions are caused by different surface-segregated substrate-related elements. The observed growth rate of ZrB_2 on sapphire was an order of magnitude higher than that on Si(111) under the same $Zr(BH_4)_4$ flux and substrate temperature. Similar increase in growth rate was observed for HfB_2 growth from the thermal decomposition of $Hf(BH_4)_4$ on molybdenum and sapphire compared to that on silicon substrate.[10] We consider that the difference in growth rates of ZrB_2 on sapphire and on Si(111) is due to the existence or lack of substrate-related elements, such as oxygen or silicon, which seems to affect the chemical reaction greatly. Under high growth rate, ZrB_2 grew on sapphire with random crystal orientation, so in order to grow ZrB_2 on sapphire with single crystal orientation, it is necessary to reduce $Zr(BH_4)_4$ flux by increasing capillary distance and/or reducing the pressure in comparison to the optimum ZrB_2 growth condition on Si(111).

III. STRUCTURAL AND ELECTRICAL CHARACTERIZATIONS

For the film grown for 60 min at 950 °C, thickness of 20 nm and B to Zr ratio of 2.0 with an accuracy of 5%, was measured using Rutherford backscattering spectroscopy. The crystalline quality and crystallographic orientation of the film was characterized by high-resolution XRD system (X'Pert PRO MRD, PANalytical) using Cu $K\alpha_1$ radiation. Figure 2(a) shows θ-2θ scan of the film. No other peak was observed besides (000*l*) peaks of sapphire substrate and ZrB_2 film. This confirms the result of RHEED, that the grown ZrB_2 film is *c*-axis oriented, i.e., the epitaxial relationship of $ZrB_2[0001]\|Al_2O_3[0001]$. High-resolution rocking curve scan for $ZrB_2(0001)$ using the triple-axis optics is shown in the inset of Fig. 2(a). Full width at half-maximum (FWHM) of the peak, 0.01°, indicates good alignment of the crystallographic planes along the *c*-axis, which is comparable to the result of ZrB_2 film on Si(111)[8] and polished ZrB_2 single crystal.[4] The *c*-axis lattice constant of ZrB_2 was estimated to be 3.526 ± 0.001 Å. Since the *c*-axis lattice constant of bulk ZrB_2 is reported to be 3.530 Å,[4] the ZrB_2 layer grown on Al_2O_3 is nearly strain-free. The in-plane orientation of ZrB_2 film respect to sapphire substrate was determined by the Φ scan. Figure 2(b) shows the Φ scan of $ZrB_2(10\bar{1}1)$ and $Al_2O_3(11\bar{2}3)$. The $Al_2O_3(11\bar{2}3)$ diffraction reveals a sixfold symmetry as expected due to its hexagonal structure. The $ZrB_2(10\bar{1}1)$ diffraction also reveals a sixfold symmetry which demonstrates that the grown ZrB_2 film has singular in-plane crystal orientation. The peak positions of the $ZrB_2(10\bar{1}1)$ planes are at the same azimuthal positions as the $Al_2O_3(11\bar{2}3)$ planes, that results in the in-plane orientation relationship of $ZrB_2[11\bar{2}0]\|Al_2O_3[10\bar{1}0]$, which is consistent with the RHEED results. The FWHM of the $ZrB_2(10\bar{1}1)$ peaks are 2.6°, which indicates good crystalline quality. Alignment of ZrB_2 and sapphire crystals provides 33% lattice mismatch, which is favorable if the growth proceeds through 3:2 magic mismatch of 0.1% between Zr-lattice and Al-lattice. But instead, we observed 30° rotation with lattice mismatch of 15%, which corresponds to 7:8 magic mismatch of 1% between Zr-lattice and O-lattice. This mismatch is comparable to that of 6:5 magic mismatch of 1% in the case of $ZrB_2(0001)$ on Si(111).[8] Aligned nucleation was only ob-

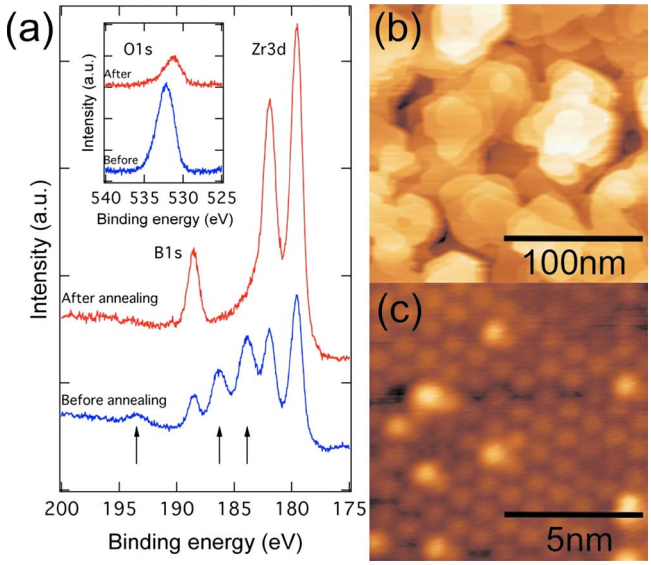

FIG. 3. (Color online) (a) XPS results for ZrB_2 film on sapphire before and after annealing at 730 °C. Oxide-related peaks of Zr 3*d* and B 1*s*, which are indicated by arrows, disappeared after the annealing. (Inset) O 1*s* peak intensity was reduced after annealing, but did not disappear, suggesting that the surface reconstruction is induced by oxygen. (b) 200×200 nm^2 scanning tunneling microscopy image of oxide removed surface, showing atomically flat terraces, observed with sample bias voltage (V_s) of 1.18 V and constant tunneling current (I) of 53.4 pA. (c) 10×10 nm^2 image of atomically resolved $ZrB_2(0001)$-(3×3), observed with $V_s=-1.57$ V and $I=135.3$ pA.

served at low growth temperature, below 900 °C, and together with 30° rotation, so we consider that the hexagonal interface matching between Zr-lattice and O-lattice, and also between Al-lattice and B-lattice, results in more stable interface allowing the observed epitaxial relationship.

The electrical resistivity was measured by standard van der Pauw method at room temperature. The lowest resistivity, 20 $\mu\Omega$ cm, was measured for a stoichiometric film with thickness of 36 nm. This value is approximately four times higher than that of ZrB_2 single crystal, presumably due to the crystal size and the thickness of the film. Nevertheless, it is comparable or even superior to the reported values of 46 $\mu\Omega$ cm (Ref. 5) and 66 $\mu\Omega$ cm,[6] reflecting high purity and high crystallinity of the obtained film.

IV. *EX SITU* SURFACE CLEANING

In order to be a good template for epitaxial growth, surface oxide should be removed easily. Similar to our earlier cleaning procedure of ZrB_2 films on Si(111),[11] we successfully cleaned ZrB_2 films on sapphire by simply heating under UHV. The samples were cut after various measurements, cleaned ultrasonically with acetone, ethanol and deionized water, and installed in our UHV scanning probe microscopy system, which is combined with x-ray photoelectron spectroscopy (XPS) and RHEED. The RHEED pattern of as-loaded samples showed spots corresponding to ZrB_2 (not shown here). As-loaded sample and sample degassed at 530 °C showed Zr–O and B–O related peaks in addition to ZrB_2-related peaks in XPS spectra measured with Mg $K\alpha$ radiation as shown in Fig. 3(a). We found that B–O peak and Zr–O peaks, which are indicated by arrows in Fig. 3(a), disappeared completely after heating the sample at 730 °C for 3 h and for overnight, respectively. XPS spectra showed no further change by heating at 780 °C for more than 10 h. After oxide-related XPS peaks at Zr 3*d* and B 1*s* region disappeared, RHEED pattern changed into streaky pattern, and $ZrB_2(0001)$-(3×3) surface reconstruction, which is different from the pattern observed during and after growth, was observed (not shown here). Oxygen 1*s* peak, which is shown in the inset of Fig. 3(a), was greatly reduced after the heat treatment, but small component at the lower binding energy side remained. This result is very different from the case of $ZrB_2(0001)$-(2×2) observed for ZrB_2 film on Si(111), which showed no O 1*s* peak after the similar heat treatment.[11] Thus, we consider that the (3×3) reconstruction in this study is induced by oxygen. Scanning tunneling microscopy was carried out on this surface, and atomically flat terraces with heights of single or multiple of *c*-lattice constant of ZrB_2 with $ZrB_2(0001)$-(3×3) structure was observed, as shown in Figs. 3(b) and 3(c). The similarity in temperature and difference in surface reconstruction suggest that the oxide reduction may be intrinsic to ZrB_2 surface, but the mechanism is still under investigation.

V. CONCLUSIONS

In summary, we demonstrated that conductive and single-crystalline ZrB_2 thin film can be grown on insulating sapphire using thermal decomposition of $Zr(BH_4)_4$ under UHV. Annealing at approximately 750 °C in UHV removes oxide from the air-exposed film, and well-defined $ZrB_2(0001)$-(3×3) surface is obtained. This metallic epitaxial ZrB_2 layer on sapphire can be used not only as a growth template and/or electrode for III-N semiconductors, but also for other hexagonal wide-gap semiconductor, such as ZnO, or diborides, such as superconducting MgB_2.

ACKNOWLEDGMENTS

This work was supported by Special Coordination Funds for Promoting Science and Technology commissioned by MEXT, Japan, and also by KAKENHI (Grant No. 19686043).

[1] F. A. Ponce and D. P. Bour, Nature (London) **386**, 351 (1997).
[2] H. Amano, N. Sawaki, I. Akasaki, and Y. Toyoda, Appl. Phys. Lett. **48**, 353 (1986).
[3] S. Nakamura, Jpn. J. Appl. Phys., Part 2 **30**, L1705 (1991).
[4] H. Kinoshita, S. Otani, S. Kamiyama, H. Amano, I. Akasaki, J. Suda, and H. Matsunami, Jpn. J. Appl. Phys., Part 2 **40**, L1280 (2001).
[5] J. Sung, D. M. Goedde, G. S. Girolami, and J. R. Abelson, J. Appl. Phys. **91**, 3904 (2002).
[6] W. Zagozdzon-Wosik, C. Darne, D. Radhakrishnan, I. Rusakova, P. van der Heide, Z.-H. Zhang, J. Bennet, L. Trombetta, P. Majhi, and D. Matron, Rev. Adv. Mater. Sci. **8**, 185 (2004).
[7] R. Khanna, K. Ramani, V. Cracium, R. Singh, S. J. Pearton, F. Ren, and I. I. Kravchenko, Appl. Surf. Sci. **253**, 2315 (2006).
[8] J. Tolle, R. Roucka, I. S. T. Tsong, C. Ritter, P. A. Crozier, A. V. G. Chizmeshya, and J. Kouvetakis, Appl. Phys. Lett. **82**, 2398 (2003).
[9] C. W. Hu, A. V. G. Chizmeshya, J. Tolle, J. Kouvetakis, and I. S. T. Tsong, J. Cryst. Growth **267**, 554 (2004).
[10] Y. Yang, S. Jayaraman, D. Y. Kim, G. S. Girolami, and J. R. Abelson, J. Cryst. Growth **294**, 389 (2006).
[11] Y. Yamada-Takamura, Z. T. Wang, Y. Fujikawa, T. Sakurai, Q. K. Xue, J. Tolle, P.-L. Liu, A. V. G. Chizmeshya, J. Kouvetakis, and I. S. T. Tsong, Phys. Rev. Lett. **95**, 266105 (2005).